Journal of Magnetism and Magnetic Materials 331 (2013) 133–139

Contents lists available at SciVerse ScienceDirect

Journal of Magnetism and Magnetic Materials

journal homepage: www.elsevier.com/locate/jmmm

Magnetic properties of quasi-one-dimensional antiferromagnets $(Y_{1-x}Nd_x)_2BaNiO_5$ ($x=1$, 0.15)

E.A. Popova [a,*], S.A. Klimin [b], M.N. Popova [b], R. Klingeler [c], N. Tristan [d], B. Büchner [d], A.N. Vasiliev [e]

[a] Moscow Institute of Electronics and Mathematics, National Research University "Higher School of Economics" 109028 Moscow, Russia
[b] Institute of Spectroscopy, RAS, 142190 Troitsk, Moscow, Russia
[c] Kirchhoff Institute for Physics, University of Heidelberg, INF 227, 69120 Heidelberg, Germany
[d] Leibniz-Institute for Solid State and Materials Research Dresden (IFW Dresden), 01171 Dresden, Germany
[e] Low Temperature Physics Department, Moscow State University, 119991 Moscow, Russia

ARTICLE INFO

Article history:
Received 27 February 2012
Received in revised form
1 November 2012
Available online 27 November 2012

Keywords:
Haldane chain
Nickelate
Chain breaks

ABSTRACT

We present the magnetic properties of $(Y_{1-x}Nd_x)_2BaNiO_5$ ($x=1$, 0.15) investigated by means of specific heat, magnetic susceptibility, and spectroscopic measurements. Magnetic ordering occurs at 47 K and 13 K in the compounds with $x=1$ and $x=0.15$, respectively. We estimate the magnetic contribution of the neodymium subsystem to magnetization and specific heat using temperature dependences of the splitting of ground Kramers doublet of Nd^{3+} ion obtained from spectroscopic experiment. We show that both Nd–Ni and Nd–Nd interactions should be taken into account. An origin of the observed spin-glass state below ~5 K and a contribution of the Ni chain breaks to the magnetization and specific heat are discussed.

1. Introduction

R_2BaNiO_5 (R=rare earth or yttrium) nickelates attract considerable interest because the magnetic properties of these compounds are associated with a strongly one-dimensional character of their structure. The crystal structure of R_2BaNiO_5 contains flattened NiO_6 octahedra sharing their corners and forming infinite chains along the a-axis which are interconnected through the R^{3+} and Ba^{2+} ions (see, e.g., [1]). Y_2BaNiO_5 is well known as a typical Haldane-gap system with a spin gap of about 10 meV in the magnetic excitation spectrum [2–4]. Doping with nonmagnetic impurities severs the NiO chains, yielding an attenuated and blue-shifted Haldane mode and new magnetic states below the Haldane gap in $Y_{2-x}Ca_xBaNi_{1-y}M_yO_5$ (M=Zn or Mg) [5–8]. Total or even partial substitution of a magnetic rare-earth ion for the nonmagnetic yttrium leads to the antiferromagnetic ordering of $(Y_{1-x}R_x)_2BaNiO_5$ at the R- and x-dependent Neel temperature [9–14]. For the stoichiometric compounds ($x=1$), the Neel temperature ranges from 12 K (R=Tm) to 61 K (R=Dy) [11–14]. In the ordered state, the magnetic structure of every R_2BaNiO_5 compound is characterized by the temperature-independent propagation vector $\mathbf{k}=(1/2,0,1/2)$ for both Ni^{2+} and R^{3+} ions [15,16], but the orientation of the Ni^{2+} and R^{3+} magnetic moments is determined by the rare-earth single-ion anisotropy [17–20]. Inelastic neutron scattering experiments on the mixed compounds $(Y_{1-x}Nd_x)_2BaNiO_5$, $x=1$, 0.75, 0.4, and 0.25, undertaken with the aim to study a crossover from the 1D quantum to the 3D classical behavior, have shown a paradoxical coexistence of the Haldane-gap excitations and spin waves in the ordered state [21–23]. This behavior has been qualitatively explained in the framework of a mean-field model that considered Haldane chains in a staggered magnetic field created by the ordered rare-earth magnetic moments [9,22,24]. Subsequent Quantum Monte Carlo study of the Hamiltonian that took into account the interaction within the $S=1$ chains (characterized by the exchange integral J) and the interaction between the chains and the rare-earth ions (characterized by the exchange integral J_c) described also the critical region near T_N, which was not possible in the mean-field approach [25,26]. A quantitative agreement with the experimental results on Nd_2BaNiO_5 and Er_2BaNiO_5 was achieved provided $J_c/J=0.3$ [25,26] and 0.2 [26], respectively. However, R–R interactions were neglected in this study and an oversimplified rather than realistic lattice pattern was used. It should also be mentioned that the value $J_c/J=0.2$ for Er_2BaNiO_5 contradicts the results of Ref. [19], where the value $J_c/J=0.07$ was obtained from the fit of the measured magnetic susceptibility vs temperature curve, using high-resolution optical data.

In the present work, magnetic properties of $(Y_{1-x}Nd_x)_2BaNiO_5$ ($x=1$, 0.15) were studied by means of spectroscopic, magnetic susceptibility, and specific heat measurements. We calculate, following the root of Ref. [19], magnetic contribution of the neodymium subsystem into magnetization and specific heat, estimate the strength of the Nd–Nd interaction, and show that

* Corresponding author.
E-mail address: eapopova@yahoo.com (E.A. Popova).

0304-8853/$ - see front matter © 2012 Elsevier B.V. All rights reserved.
http://dx.doi.org/10.1016/j.jmmm.2012.11.019

this interaction is essential for a quantitative explanation of the magnetic susceptibility and specific heat of both compounds studied. The influence of uncontrolled impurities on the low-temperature magnetization and specific heat as well as manifestations of intrinsic features of the Haldane chain are discussed.

2. Experiment

Polycrystalline samples of $(Y_{1-x}Nd_x)_2BaNiO_5$ with $x=1.0$ and 0.15 were synthesized by solid state reactions [14]. The quality and composition of the samples were tested by X-ray diffraction techniques. Temperature dependences of the magnetization in zero-field-cooled (ZFC) and field-cooled (FC) regimes were measured in the magnetic field of 0.01 T at temperatures between 1.8 and 350 K using a MPMS-XL5 SQUID magnetometer (Quantum Design). Temperature dependences of the specific heat were studied in the temperature range 0.4–300 K by means of a relaxation method in a Physical Property Measurement System (Quantum Design). Optical absorption measurements in the spectral range 10,000–15,000 cm^{-1} were performed using a Fourier spectrometer BOMEM DA3.002.

3. Results

Fig. 1 shows temperature dependences of the magnetic susceptibility $\chi(T)$ measured in the magnetic field of $B=0.01$ T in ZFC and FC regimes for $(Y_{1-x}Nd_x)_2BaNiO_5$ compounds with $x=1$ and $x=0.15$. Fig. 2 presents experimental data on the specific heat $C(T, B=0)$ of the same compounds. The value of the magnetic susceptibility depends on the neodymium concentration. At high temperatures, the magnetic susceptibility of both compounds demonstrates a Curie-like behavior. For Nd_2BaNiO_5, both a λ-type anomaly in the $C(T)$ dependence and a kink in the $\chi(T)$ dependence manifest an antiferromagnetic phase transition. The temperature of this transition, $T_N=47$ K, is in a good agreement with neutron scattering [9] and earlier spectroscopic [11,18] data. A broad maximum named the Schottky anomaly, observed in both $C(T)$ and $\chi(T)$ dependences below T_N originates from the temperature-driven depopulation of upper component of the Nd^{3+} ground Kramers doublet split in an internal magnetic field that appears in the magnetically ordered state. A broad maximum in the $\chi(T)$ dependence shifts to lower temperatures with decreasing neodymium concentration. In the compound with $x=0.15$, we observed only one anomaly in the $C(T)$ dependence, with irregular shape. We assume that the temperature of the λ-type anomaly approaches the temperature of the maximum of the Schottky anomaly. This assumption is based on the fact that the Schottky anomaly is a broad maximum with a gradual decreasing of the specific heat above the temperature of the maximum. However, in the experiment we observed a sharp drop of the specific heat above T_{max}. An additional maximum in the $\chi(T)$ dependence is observed at about 3 K for both compounds. Fig. 1b demonstrates the difference in the behavior of the magnetic susceptibility measured in ZFC and FC regimes, below 5 K. Such difference is typical for a spin-glass state.

In order to calculate the contribution of the Nd subsystem to magnetic susceptibility and specific heat we performed the study of absorption spectra corresponding to optical transitions from the ground state ($^4I_{9/2}$) to the excited states of the $4f^3$ electronic configuration of the Nd^{3+} ion. As the 4f shell is well shielded from the environment by the filled 5s and 5p shells, the energy levels of Nd^{3+} in a crystal do not differ much from those of a free Nd^{3+} ion and the crystal field can be considered as a perturbation. In the crystal lattice of the title compounds, neodymium occupies a single position characterized by the C_{2v} point symmetry group. The C_{2v} symmetry crystal field splits a Nd^{3+} free-ion level with a total momentum J into $J+1/2$ Kramers doublets. In particular, the ground state $^4I_{9/2}$ splits into five Kramers doublets but the excited state $^4F_{3/2}$ located at about 11,200 cm^{-1} splits into two Kramers doublets (see the scheme in Fig. 3a). Fig. 3b shows the absorption spectra of Nd_2BaNiO_5 at different temperatures in the region of an optical transition between the ground Kramers doublet and the lowest level of the $^4F_{3/2}$ crystal-field multiplet. At elevated temperatures, only one line is observed corresponding to the line

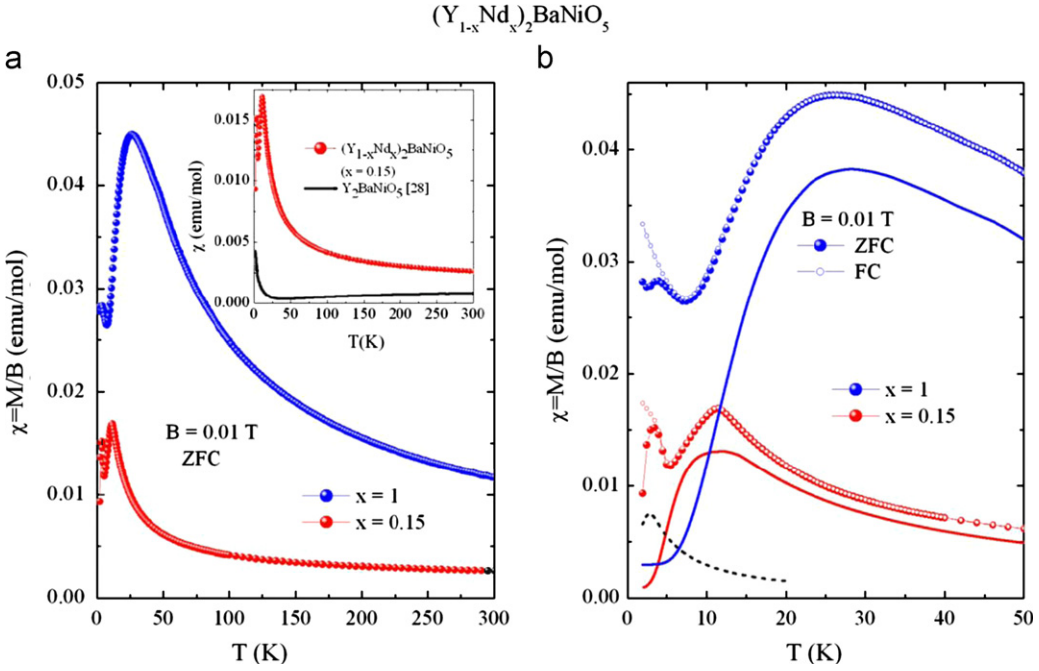

Fig. 1. Temperature dependences of the magnetic susceptibility $\chi(T)$ of $(Y_{1-x}Nd_x)_2BaNiO_5$ compounds with $x=1$ and $x=0.15$, measured in a magnetic field of $B=0.01$ T (a) in ZFC regime and (b) in ZFC and FC regimes (the low-temperature region up to 70 K is displayed). In both plots, experimental data are shown by closed circles (ZFC) and open circles (FC). Solid and dashed lines show the contribution of the Nd and Ni subsystems, respectively (see the text). Inset compares $\chi(T)$ of $(Y_{1-x}Nd_x)_2BaNiO_5$, $x=0.15$, and of a nominally pure Y_2BaNiO_5 [28].

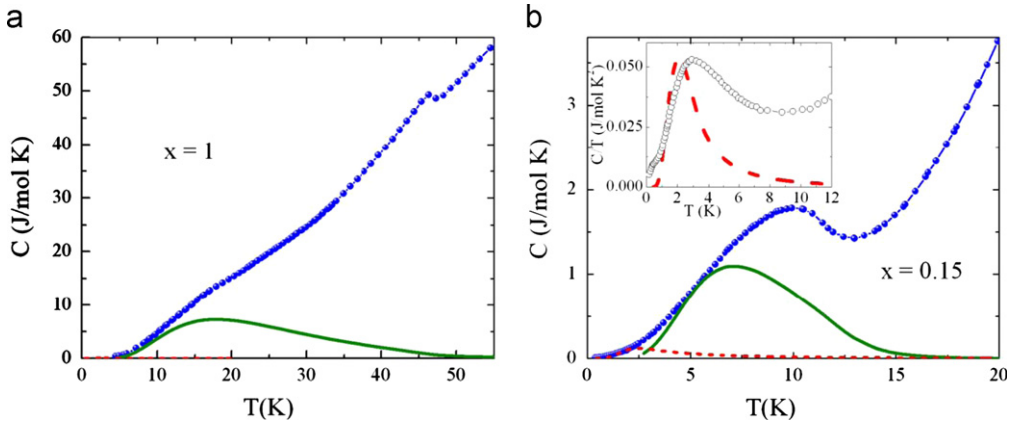

Fig. 2. Temperature dependences of the specific heat $C(T)$ of $(Y_{1-x}Nd_x)_2BaNiO_5$ compounds with (a) $x=1$ and (b) $x=0.15$, measured in zero magnetic field. Experimental data are represented by symbols. Solid and dashed lines show contributions of the Nd and Ni subsystems, respectively (see the text). Inset: dashed line corresponds to the contribution of the Ni subsystem to $C(T)$ of $(Y_{1-x}Nd_x)_2BaNiO_5$, open symbols display the experimental data for $Y_2BaNi_{0.96}Zn_{0.04}O_5$ ($B=6$ T) taken from Ref. [5].

marked IA in the scheme of Fig. 3a. At 61 K, this is the spectral line 11,190 cm^{-1} in Fig. 3b. A well resolved splitting of this line observed with lowering temperature in the absence of an external magnetic field (see Fig. 3b, spectral traces for $T=28$ and 5 K) points unambiguously to a presence of an internal magnetic field that appears in a magnetically ordered state and splits the Nd^{3+} Kramers doublets (note that the Kramers degeneracy cannot be removed by any perturbation except a magnetic field). Four lines clearly seen in Fig. 3b for $T=28$ K correspond to the lines marked 1′a, 1′a′, 1a, and 1a′ in the scheme of Fig. 3a. The low-frequency lines 1′a and 1′a′ vanish with decreasing temperature, due to emptying of the initial state of the corresponding transitions. A value of the splitting Δ of the ground Kramers doublet is determined as the distance between two spectral lines corresponding to transitions from two split sublevels of the ground state to the same final state (see Fig. 3b). To find Δ for the temperatures below 10 K, interpolation was used (we note that the central frequency $\omega_0=\omega(1a')-\omega(1'a)=\omega(1a)-\omega(1'a')$ does not depend on temperature). In the mixed nickelates, non-equivalent rare-earth centers exist, due to the Nd–Y disorder in the nearest surrounding of a given Nd^{3+} ion. This leads to a spectral line broadening and a complex line shape in the compound with $x=0.15$ [27]. No separate spectral components are resolved even at the lowest temperature; meanwhile the spectral weight demonstrates the gradual shift to the high-frequency part upon cooling. Change in the shape of the neodymium spectral lines with decreasing temperature and the Schottky anomalies in the $C(T)$ and $\chi(T)$ dependences point to the appearance of an internal magnetic field in the compound with $x=0.15$. The splitting Δ of the ground Kramers doublet of the Nd^{3+} ion in the compound with $x=0.15$ was determined from the position of center of mass of the spectral line against the baseline. This baseline was derived by interpolating down to the lowest temperature the position of the spectral line in paramagnetic range, as shown in the inset of Fig. 3c. Temperature dependences of the Nd^{3+} ground Kramers doublet splitting obtained from spectroscopic measurements for the compounds studied are shown in Fig. 4. The splitting, and hence the internal magnetic field acting on the Nd^{3+} ion, increases with decreasing temperature. The point of inflection in the $\Delta(T)$ curve corresponds to the antiferromagnetic phase transition [10].

4. Discussion

The magnetic system of $(Y_{1-x}Nd_x)_2BaNiO_5$ consists of two kinds of magnetic ions, namely, Ni^{2+} ($S=1$) and Nd^{3+} ($S=3/2$, $L=6$, $J=9/2$), which contribute to the magnetic properties. We have found some common features in magnetic behavior of the compounds studied. Above $T=100$ K, the magnetic susceptibility of both compounds demonstrates a Curie–Weiss like behavior. The theoretical value of effective magnetic moment of both Nd^{3+} and Ni^{2+} ions in $(Y_{1-x}Nd_x)_2BaNiO_5$ is defined by the formula $\mu_{eff}(x)=\mu_B\sqrt{2xg_J^2J(J+1)+g_S^2S(S+1)}$, where μ_B is the Bohr magneton, $g_J=8/11$ is the ground-state Lande factor for the Nd^{3+} ion, and $g_S=2$ for the Ni^{2+} ion. The factor $2x$ takes into account concentration of the neodymium ions in the compound. Fitting experimental data for the compound with $x=1$ yields the effective magnetic moment $\mu_{eff}=5.06\mu_B$ which is close to the free-ion value $\mu_{eff}=\sqrt{2g_J^2J(J+1)}\mu_B=5.12\mu_B$ for Nd^{3+} in Nd_2BaNiO_5 with two neodymium ions per formula unit and smaller than the value $\mu_{eff}=5.85\mu_B$ obtained when taking into account the $S=1$ spin for Ni^{2+}. Therefore, contribution of the nickel subsystem to magnetic susceptibility is negligible in the high-temperature range. This could be explained if the behavior of the nickel subsystem in Nd_2BaNiO_5 was similar to that in the isostructural Y_2BaNiO_5 compound. Indeed, neutron scattering experiments have revealed an energy gap of about 11 meV in the magnetic excitation spectrum of nickel chains above the Neel temperature for all members of the system $(Y_{1-x}Nd_x)_2BaNiO_5$ ($x=1$, 0.75, 0.5, 0.25) [9], which is in favor of the above assumption. We assume that the Haldane-gap state of the nickel chain is also preserved in the high-temperature range for the compound with $x=0.15$. Above 100 K, the magnetic susceptibility of the Nd subsystem decreases with increasing temperature, while the magnetic susceptibility of Ni subsystem being in Haldane gap state increases with heating (see the inset of Fig. 1(a)). For the compound with $x=1$, a behavior of the total magnetic susceptibility is governed, mainly, by the Nd subsystem because the value of the magnetic susceptibility of Ni subsystem is much smaller than that of the Nd subsystem (see Fig. 1(a) and its inset). For the compound with $x=0.15$, contribution of the Ni subsystem begins to play a bigger role and therefore the behavior of total magnetic susceptibility of $(Y_{0.85}Nd_{0.15})_2BaNiO_5$ is not well described by the Curie–Weiss law, namely, the value of the effective magnetic moment for the compound with $x=0.15$ depends on the temperature range of fitting. After subtracting the magnetic susceptibility of nickel subsystem taken from Ref. [28] for Y_2BaNiO_5 (see inset of Fig. 1(a)), we get an estimate for the effective magnetic moment $\mu_{eff}=1.81\mu_B$ for $(Y_{0.85}Nd_{0.15})_2BaNiO_5$. This value is almost independent of the fitting temperature range and is close to the free-ion value $\mu_{eff}=\sqrt{2\times0.15g_J^2J(J+1)}\mu_B=1.98\mu_B$ for Nd^{3+} in this compound.

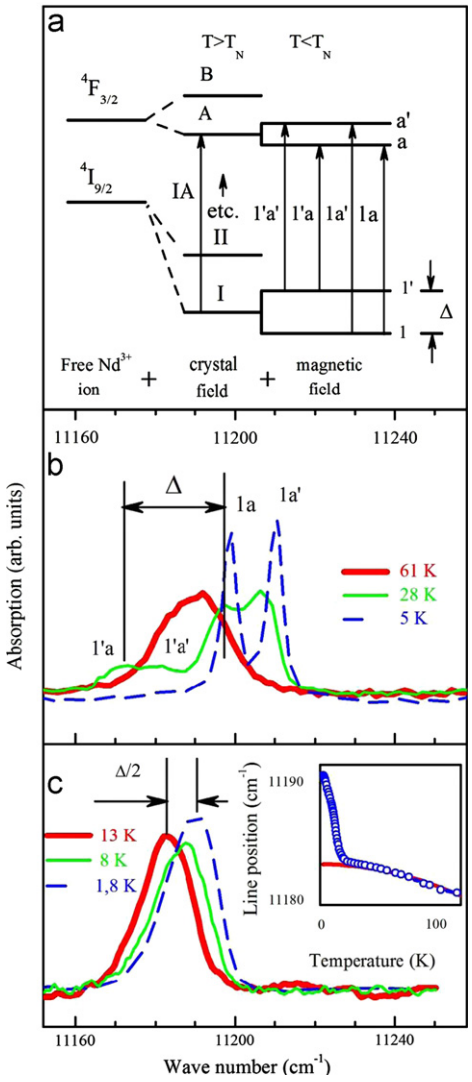

Fig. 3. Absorption spectra of $(Y_{1-x}Nd_x)_2BaNiO_5$ at different temperatures in the region of the $^4I_{9/2} \rightarrow {}^4F_{3/2}$ optical transition of Nd^{3+}: (a) schematic representation (see the text); (b) $x=1$ and (c) $x=0.15$. Inset: temperature dependence of the mass center position of the spectral line. Solid line displays the mass center position interpolated from the paramagnetic range to the low-temperature range for the compound with $x=0.15$.

So, we argue that the Haldane-gap state of the nickel chains is preserved in the high-temperature range for the studied mixed compounds $(Y_{1-x}Nd_x)_2BaNiO_5$. The Curie–Weiss fitting of the magnetic susceptibility results in negative Weiss temperatures $\Theta_{x=1} \approx -43$ K and $\Theta_{x=0.15} \approx -33$ K for the compounds with $x=1$ and $x=0.15$, respectively, which points to a predominance of antiferromagnetic exchange interactions. The absolute value of the Weiss temperature decreases with decreasing neodymium concentration in $(Y_{1-x}Nd_x)_2BaNiO_5$, indicating weakening of antiferromagnetic interactions which is natural for a magnetically diluted system.

To calculate contributions of the Nd subsystem to the magnetic susceptibility and specific heat, the data on the Nd^{3+} levels obtained from spectroscopic measurements were used. The energies of the Nd^{3+} crystal-field levels in $(Y_{1-x}Nd_x)_2BaNiO_5$ depend little on x. Because the second Kramers doublet is situated at 140 cm^{-1} above the ground doublet for both compounds studied [29], magnetic properties of the compounds below the temperature ~50 K are governed by the ground Kramers doublet, as all other states are depopulated. In a magnetically ordered state ($T < T_N = 47$ K), the splitting $\Delta(T)$ of the ground Kramers doublet has to be taken into

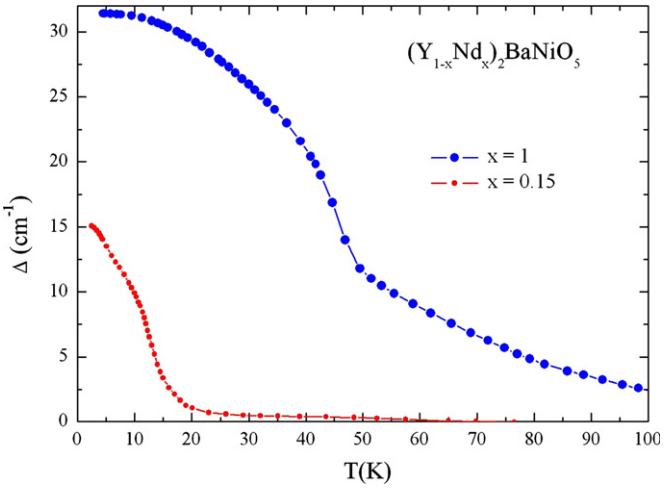

Fig. 4. Temperature dependences of the splitting $\Delta(T)$ of the ground Kramers doublet of the Nd^{3+} ion estimated from spectroscopic data for $(Y_{1-x}Nd_x)_2BaNiO_5$ compounds with $x=1$ and $x=0.15$.

account. When modeling the experimental data on the magnetic susceptibility and specific heat, we used the values of $\Delta(T)$ found from the spectra. They are shown in Fig. 4. The observed $\Delta(T)$ decreases with decreasing x, which results in a reduced magnetic moment of both the neodymium and nickel subsystems.

To fit the experimental data, Nd–Ni and Nd–Nd interactions were considered. The effective magnetic field acting on Nd^{3+} results from both an external field B and an internal field. The latter one is created, mainly, by the nickel subsystem and is, mainly, due to the Nd–Ni (f–d) exchange interaction. In addition, we take also the Nd–Nd interaction into account. The effective magnetic field splits the ground state of the Nd^{3+} ion into two sublevels. Energies of these sublevels can be written as

$$E = \pm \frac{1}{2}\Delta_{1,2}, \tag{1}$$

$$\Delta_{1,2} = \mu_B \sqrt{g_a^2 B_{\mathrm{eff}1,2a}^2 + g_b^2 B_{\mathrm{eff}1,2b}^2 + g_c^2 B_{\mathrm{eff}1,2c}^2} \tag{2}$$

Here, $g_a=0.36$, $g_b=0.94$, and $g_c=5.4$ are the components of the g-tensor of the Nd^{3+} ground state in Nd_2BaNiO_5 [18] and $B_{\mathrm{eff}1,2\alpha}$ ($\alpha=a, b, c$) are the components of the effective magnetic field. As follows from the neutron scattering experiments on $(Y_{1-x}Nd_x)_2BaNiO_5$, both nickel and rare-earth subsystems can be considered in the two-sublattice approximation. Magnetic moments of the Ni^{2+} ions lie in the ac-plane of the crystal forming an angle $\gamma=35^\circ$ with the c-axis. These neutron scattering data refer to the compounds with $x=1$, 0.75, 0.5, 0.25 [9]. We use them also for the compound with $x=0.15$. Indices 1 and 2 represent the neodymium sublattices, named the I and the II sublattices, for which the component of the field created by the nickel subsystem, $B_{ex\alpha}$, is oriented along or opposite to the direction of an external field B, respectively. Below T_N, Nd^{3+} ions with opposite directions of the magnetic moments are not equivalent in the presence of an external magnetic field $B \| \alpha$, and the effective fields acting on the Nd^{3+} ions are [19]

$$\begin{cases} B_{\mathrm{eff}1\alpha} = B + \kappa_{11\alpha} M_{1\alpha}^{\mathrm{Nd}} + \kappa_{12\alpha} M_{2\alpha}^{\mathrm{Nd}} + B_{\mathrm{ex}\,\alpha} \\ B_{\mathrm{eff}2\alpha} = B + \kappa_{11\alpha} M_{2\alpha}^{\mathrm{Nd}} + \kappa_{12} M_{1\alpha}^{\mathrm{Nd}} - B_{\mathrm{ex}\,\alpha} \end{cases} \tag{3}$$

Here, $M_{1\alpha}^{\mathrm{Nd}}$ and $M_{2\alpha}^{\mathrm{Nd}}$ are the components of the magnetic moments of the I and the II neodymium sublattices, respectively. Parameters κ_{11} and κ_{12} determine internal magnetic fields acting on the Nd^{3+} ion with the magnetic moments which are induced by Nd^{3+} ions with the same (κ_{11}) and opposite (κ_{12}) directions of

their magnetic moments. Expanding the magnetic moments of neodymium ions, $M^{Nd}_{1,2\alpha}$, in the effective magnetic fields (3) in powers of the differences$(B_{eff1\alpha}-(B+B_{ex\alpha}))$ and $(B_{eff2\alpha}-(B-B_{ex\alpha}))$ for the I and the II neodymium sublattices, respectively, we obtain the following relations for the components of the magnetic moments:

$$M^{Nd}_{1\alpha}=\frac{M^{-}_{0\alpha}\kappa_{12\alpha}\chi^{+}_{\alpha\alpha}+M^{+}_{0\alpha}(1-\kappa_{11\alpha}\chi^{-}_{\alpha\alpha})}{(1-\kappa_{11\alpha}\chi^{-}_{\alpha\alpha})(1-\kappa_{11\alpha}\chi^{+}_{\alpha\alpha})-\kappa^{2}_{12\alpha}\chi^{-}_{\alpha\alpha}\chi^{+}_{\alpha\alpha}} \quad (4)$$

$$M^{Nd}_{2\alpha}=\frac{M^{+}_{0\alpha}\kappa_{12\alpha}\chi^{-}_{\alpha\alpha}+M^{-}_{0\alpha}(1-\kappa_{11\alpha}\chi^{+}_{\alpha\alpha})}{(1-\kappa_{11\alpha}\chi^{-}_{\alpha\alpha})(1-\kappa_{11\alpha}\chi^{+}_{\alpha\alpha})-\kappa^{2}_{12\alpha}\chi^{-}_{\alpha\alpha}\chi^{+}_{\alpha\alpha}} \quad (5)$$

Here, $M^{\pm}_{0\alpha}$ and $\chi^{\pm}_{\alpha\alpha}$ are the components of the magnetic moments and of the magnetic susceptibility, respectively, in the effective field $\vec{B}_{eff}=\vec{B}+\vec{B}_{ex}$. Sign "+" refers to the I neodymium sublattice, sign "−" corresponds to the II sublattice. $M^{\pm}_{0\alpha}$ is calculated by differentiating Eq. (1) with respect to the components of the effective magnetic field, assuming the Boltzmann distribution of electrons on the energy sublevels of the Nd^{3+} ion:

$$M^{\pm}_{0\alpha}=2x\frac{g_{\alpha}{}^{2}B_{eff\alpha}\mu_B^2}{2\Delta_{1,2}}\,\mathrm{th}\left(\frac{\Delta_{1,2}}{2kT}\right), \quad (6)$$

where k is the Boltzmann constant. The factor $2x$ takes into account the concentration of the neodymium ions in the compound. Here, $\Delta_{1,2}$ are calculated with Eq. (2) using appropriate B_{eff}. Thus, in the case of an external field B parallel to the a-axis, $B\|a$, components of the effective field are $B_{effa}=B\pm B_{exa}$; $B_{effb}=\pm B_{exb}$; $B_{effc}=\pm B_{exc}$. Analogous expressions are valid also for other directions of the external magnetic field. Components of the magnetic susceptibility are calculated by differentiating Eq. (6) with respect to the external magnetic field:

$$\chi^{\pm}_{\alpha\alpha}=\left.\frac{\partial M^{\pm}_{0\alpha}}{\partial B}\right|_{\vec{B}_{eff}=\vec{B}+\vec{B}_{ex}}.$$

The components of the total magnetization can be described as a superposition of two contributions, $M_{\alpha}=0.5(M_{1\alpha}+M_{2\alpha})$, where each contribution corresponds to one of the two neodymium sublattices with appropriate B_{eff}. The magnetic susceptibility of a polycrystalline sample is $\chi=N_A\sum_{\alpha=a,b,c}M_{\alpha}/3B$.

The Schottky anomaly in the $C(T)$ dependence results from a temperature-driven repopulation of the ground-state sublevels of the Nd^{3+} ion, and the contribution of both neodymium sublattices can be written as

$$C_{1,2}=2xR\left(\frac{\Delta_{1,2}}{kT}\right)^{2}\frac{\exp(\Delta_{1,2}/kT)}{\left(1+\exp(\Delta_{1,2}/kT)\right)^{2}}, \quad (7)$$

where R is the gas constant.

Contributions of the neodymium subsystem into the magnetic susceptibility $\chi(T)$ and specific heat $C(T)$ are shown by solid lines in Figs. 1b and 2, respectively. The fitting parameters $\kappa_{11z}=-1.62$ mol/emu, $\kappa_{12z}=-1.3$ mol/emu provide the best agreement with the experimental data for both compounds. Other components of the parameters κ_{11} and κ_{12} have little influence on the fitting. This fact reflects the strong anisotropy of magnetic properties of the compounds studied. The values of fitted parameters κ_{11} and κ_{12} exceed $\kappa_{11}=\kappa_{12}=-0.0451$ T/$\mu_B=-0.081$ mol/emu estimated for the polycrystalline sample of Er_2BaNiO_5 [19]. This might be caused by a difference in ionic radii of Nd^{3+} and Er^{3+} leading to an enhanced exchange interaction in the case of Nd_2BaNiO_5 as compared to Er_2BaNiO_5. If one neglects the Nd–Nd interactions (i.e. $\kappa_{11}=\kappa_{12}=0$), the calculated Nd contribution to the magnetic susceptibility considerably exceeds the experimental results, whereas the calculated Schottky anomaly in the magnetic susceptibility noticeably shifts with respect to the experimental results. Thus, the Nd–Nd interactions are important in the case of Nd_2BaNiO_5 and should be included. The difference between κ_{11} and κ_{12} could be ascribed to a difference in the exchange pathways. In the crystal structure of R_2BaNiO_5, the neodymium sites are positioned between the nickel chains. The Nd^{3+} spins form a network via Ni–O–Nd and Nd–O–Nd superexchange routes. Along the b-axis, magnetic moments of the two Nd^{3+} ions interact with each other via the same $d_{x^2-y^2}$ orbital of the Ni^{2+} ion through the Nd–O–Ni–O–Nd route. Antiferromagnetic superexchange interaction NiO–Nd leads to the same orientation of the magnetic moments of the Nd^{3+} ions. This effective Nd–Nd interaction is described by the parameter κ_{11}. Parameter κ_{12} determines the Nd–Nd interaction through two kinds of the routes. One of them is a long route Nd–O–Ni–O–Ni–O–Nd including two Ni^{2+} ions along the spin chain. Strong antiferromagnetic interaction between the Ni^{2+} ions inside the chain leads to the opposite orientations of the Nd $^{3+}$ magnetic moments. Another route through apical O^{2-} ion of NiO_6 octahedra also causes Nd–Nd antiferromagnetic interaction.

Taking the experimental values of $\Delta(T)$ and the calculated values of the g-factors, we can estimate internal magnetic field acting on the Nd^{3+} ions, $B_{ex}(T)$. For the lowest temperature, $B_{ex\ x=1}\approx 15.2$ T and $B_{ex\ x=0.15}\approx 8.6$ T. The $B_{ex}(T)$ dependences and the fitting parameters κ_{11}, κ_{12} were used to calculate the values of the magnetic moments of the Nd^{3+} ions for the compounds with $x=1$ and $x=0.15$ which are shown in Fig. 5. For Nd_2BaNiO_5, the calculated magnetic moments are in a good agreement with neutron scattering data taken from Ref. [9]. Note that the value of the magnetic moment of the Nd^{3+} ion is reduced for both compounds. This is typical for low-dimensional systems.

The Schottky anomaly in both $\chi(T)$ and $C(T)$ dependences is reasonably well described by the contribution of the Nd subsystem. At low temperatures, however, both $\chi(T)$ and $C(T)$ dependences demonstrate a more complex behavior. First, below 5 K, the magnetic susceptibility measured in ZFC and FC regimes differs. This is a signature of the spin-glass state. Second, the magnetic susceptibility measured in the ZFC regime exhibits a maximum at about 3 K for both compounds. The value and position of this maximum are almost independent of the concentration of the neodymium ions in the compound. Note that there is no sharp anomaly in the specific heat data indicating a phase transition at this temperature (see Fig. 2). At the same time, Fig. 2b clearly shows that the contribution of the Nd subsystem cannot describe the experimental $C(T)$ dependence in the low-temperature range ($T<5$ K), where the contribution from the

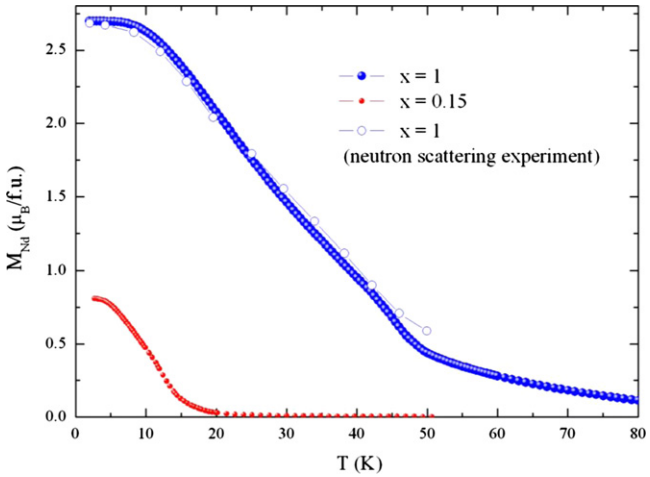

Fig. 5. Temperature dependences of the magnetic moment of the Nd^{3+} ion estimated from experimental data for $(Y_{1-x}Nd_x)_2BaNiO_5$ compounds with $x=1$ and $x=0.15$ (see the text). Open symbols display the magnetic moment of the Nd^{3+} ion for the compound with $x=1$ taken from Ref. [9] (neutron scattering experiment).

rare-earth system is negligible. These facts lead us to the conclusion that there is some additional low-temperature contribution of the nickel subsystem to the magnetic susceptibility and specific heat of the chain nickelates $(Y_{1-x}Nd_x)_2BaNiO_5$.

A similar behavior of the magnetic susceptibility and specific heat at low temperatures was observed in a nominally pure and doped Y_2BaNiO_5 compounds. In a nominally pure compound and in both cases of Ca^{2+} impurities substituting for Y^{3+} and of nonmagnetic Zn^{2+} and Mg^{2+} impurities substituting for Ni^{2+}, the Schottky anomaly in the specific heat appears in a magnetic field, and it shifts to higher temperatures with increasing field [5,30]. In addition, in the case of the off-chain Ca^{2+} impurities the maximum observed in ac-susceptibility shifts with increasing frequency and a spin-glass state is confirmed by a difference between the magnetic susceptibilities measured in ZFC and FC regimes [31]. In contrast, for in-chain doped compounds, the maximum observed in ac-susceptibility is independent of frequency [32]. X-ray absorption spectroscopy measurements show that Ca-doping creates holes which occupy both O 2*p* and Ni 3*d* orbitals along the Ni chain [33]. Formally, the Ca-doping leads to the formation of Ni^{3+} ions, which could really appear in $(Y_{1-x}Nd_x)_2BaNiO_5$ as a result of a small oxygen non-stoichiometry. The holes inside the Ni chain could induce ferromagnetic bonds between the nearest nickel ions, as in the case of Ca-doped Y_2BaNiO_5 [34]. The spin-glass state could result from a competition of the ferromagnetic and antiferromagnetic interactions.

To describe the effect of nonmagnetic doping on the bulk responses of Y_2BaNiO_5, a model is used in which nonmagnetic impurities in the $S=1$ chain produce an ensemble of finite-length chain segments. On the one hand, the maximum in magnetic susceptibility is well described [32] by inter- and intra-chain interactions of localized spins S=1/2 which result from the broken valence-bond-solid (VBS) state at the chain ends [35]. On the other hand, the Schottky anomaly in specific heat is better described [5] by a simple model involving $S=1$ excitations, instead of the $S=1/2$ excitations of the VBS. In our case, the presence of nickel-chain breaks in a nominally pure $(Y_{1-x}Nd_x)_2BaNiO_5$ can be due to uncontrolled impurities. We have made an attempt to estimate the contribution of the Ni subsystem associated with the chain breaks in two ways. In the framework of the VBS model, the $S=1/2$ localized at the ends of the chain segments interact with each other along the chain, and this interaction depends on length of the segment; it is antiferromagnetic for even segments, and ferromagnetic for odd ones [36]. We assume additionally that $S=1/2$ can be coupled via indirect exchange interaction through the Nd^{3+} ions. The localized composite $S=1/2$ degrees of freedom generate a singlet state, which does not contribute to the magnetic susceptibility and specific heat, and a triplet state. The triplet state split by both an internal and an external magnetic field contributes to the total magnetic susceptibility and specific heat.

The other way of estimation suggested in Ref. [5]is based on the idea that the even chain segments are in a singlet state, whereas odd segments are in a triplet state originating from an extra spin $S=1$. Both estimations with a number of the chain breaks ~2% give the same behavior of the magnetic susceptibility and specific heat, and are presented by dashed lines in Figs. 1b and 2, respectively. We have assumed the magnetic *g*-factor values $g_x=g_y=g_z=2.2$ for the nickel ions. At low temperatures, the behavior of both $\chi(T)$ and $C(T)$ dependences is well described by the contribution of the Ni subsystem associated with chain breaks. We note that the temperature of the maximum ~3 K in $\chi(T)$ and ~2.5 K in $C(T)$ for $(Y_{1-x}Nd_x)_2BaNiO_5$ is higher than the corresponding temperatures of 0.16 K in ac-susceptibility and of ~1.5 K in $C(T, B=3\,T)$ for $Y_2BaNi_{1-y}Zn_yO_5$ with $y=0.08$ [32] and $y=0.04$ [5], respectively. This happens, evidently, due to existence of a sufficiently high staggered magnetic field created by the Nd subsystem in the ordered state of $(Y_{1-x}Nd_x)_2BaNiO_5$. In addition, as was shown by EPR [28,37], NMR [38], and neutron scattering measurements [8], there is a staggered magnetization at impurities, which decays exponentially toward the bulk. We assume that both these processes form a spin-glass state below ~5 K (this temperature being the branching temperature between ZFC and FC data). This results in a growing internal magnetic field in the ordered state with further lowering of temperature. To account for the observed low-temperature anomalies, this field should be as large as 7 T at zero temperature (compare with the Ni–Ni exchange field within the nickel chain $B_{ex}^{Ni} \approx 230$ T, estimated from the relation $kJ_{Ni-Ni}=g\mu_B B_{ex}^{Ni}$, where $J_{Ni-Ni} \approx 300$ K [9]). Inset of Fig. 2b compares the contribution of the Ni subsystem to $C(T)$ of $(Y_{1-x}Nd_x)_2BaNiO_5$ with the experimental data for $Y_2BaNi_{0.96}Zn_{0.04}O_5$ ($B=6$ T) taken from Ref. [5]. For both curves, the positions of maxima are close to each other. A difference in the shape of the maxima results, probably, from a different kind of magnetic field acting on the Ni subsystem in both cases. The nickel subsystem of $(Y_{1-x}Nd_x)_2BaNiO_5$ is in a staggered magnetic field of about 7 T ($T=0$ K) which decreases with increasing temperature, while the uniform magnetic field of 6 T acts on the Ni subsystem of $Y_2BaNi_{0.96}Zn_{0.04}O_5$ [5]. Thus, defects of the crystal structure allow us to reveal intrinsic features of the nickel chain. Peculiarities in $\chi(T)$ and $C(T)$ associated with defects indicate that the nickel subsystem of $(Y_{1-x}Nd_x)_2BaNiO_5$ in the ordered state has the same properties that disordered nickel Haldane chains of Y_2BaNiO_5 have.

5. Conclusions

In summary, we investigated magnetic properties of $(Y_{1-x}Nd_x)_2BaNiO_5$ ($x=1$, 0.15) by means of specific heat, magnetic susceptibility, and spectroscopic measurements. A magnetic ordering occurs at 47 and 13 K in the compounds with $x=1$ and $x=0.15$, respectively. We estimate magnetic contribution of the neodymium subsystem to magnetization and specific heat using temperature dependences of the splitting of the ground Kramers doublet of the Nd^{3+} ion obtained from spectroscopic measurements and show that macroscopic, magnetic and thermodynamic properties cannot be accounted for without considering the Nd–Nd interactions. At high temperatures, while the contribution of the Nd subsystem to magnetic susceptibility follows the Curie-Weiss law, the Ni subsystem behaves like a Haldane system, the contribution of which is independent of the concentration *x*. In the low-temperature range, a spin-glass state is observed. Our study of defect-associated features in the low-temperature $\chi(T)$ and $C(T)$ dependences for $(Y_{1-x}Nd_x)_2BaNiO_5$, in comparison with literature data on Y_2BaNiO_5 doped with nonmagnetic impurities shows that the nickel chains in magnetically ordered mixed-spin $(Y_{1-x}Nd_x)_2BaNiO_5$ compounds have the same properties as those in a disordered Haldane-gap Y_2BaNiO_5 system.

Acknowledgments

Support of the Russian Foundation for Basic Research (Grant No 12–02–00858-a) and of the Russian Academy of Sciences under the Programs for Basic Research is acknowledged. RK, NT, and BB acknowledge support from the DFG via KL 1824/2.

References

[1] E. Garcria-Matres, J.L. Martínez, J. Rodríguez-Carvajal, J.A. Alonso, A. Salinas-Sánchez, R. Sáez-Puche, Journal of Solid State Chemistry 103 (1993) 322.

[2] R. Sáez-Puche, J.M. Corondo, C.L. Otero-Díaz, J.M. Martín-Llorente, Journal of Solid State Chemistry 93 (1991) 461.
[3] J. Darriet, L.P. Regnault, Solid State Communications 86 (1993) 409.
[4] K. Kojima, A. Keren, L.P. Le, G.M. Luke, B. Nachumi, W.D. Wu, Y.J. Uemura, K. Kiyono, S. Miyasaka, H. Takagi, S. Uchida, Physical Review Letters 74 (1995) 3471.
[5] A.P. Ramirez, S.-W. Cheong, M.L. Kaplan, Physical Review Letters 72 (1994) 3108.
[6] J.F. DiTusa, S.-W. Cheong, J.-H. Park, G. Aeppli, C. Broholm, C.T. Chen, Physical Review Letters 73 (1994) 1857.
[7] G. Xu, G. Aeppli, M.E. Bisher, C. Broholm, J.F. DiTusa, C.D. Frost, T. Ito, K. Oka, R.L. Paul, H. Takagi, M.M.J. Treacy, Science (New York, NY) 289 (2000) 419.
[8] M. Kenzelmann, G. Xu, I.A. Zaliznyak, C. Broholm, J.F. DiTusa, G. Aeppli, T. Ito, K. Oka, H. Takagi, Physical Review Letters 90 (2003) 087202.
[9] T. Yokoo, S.A. Raymond, A. Zheludev, S. Maslov, E. Ressouche, I. Zaliznyak, R. Erwin, M. Nakamura, J. Akimitsu, Physical Review B 58 (1998) 14424.
[10] E.A. Popova, A.N. Vasil'ev, S.A. Klimin, M.V. Narozhnyi, M.N. Popova, Journal of Experimental and Theoretical Physics 111 (2010) 204.
[11] G.G. Chepurko, Z.A. Kazei, D.A. Kudrjavtsev, R.Z. Levitin, B.V. Mill, M.N. Popova, V.V. Snegirev, Physics Letters A 157 (1991) 81.
[12] E. Garcria-Matres, J.L. Garcia-Muñoz, J.L. Martínez, J. Rodríguez-Carvajal, Journal of Magnetism and Magnetic Materials 149 (1995) 363.
[13] A. Zheludev, J.M. Tranquada, T. Vogt, D.J. Buttrey, Europhysics Letters 35 (1996) 385.
[14] V. Sachan, D.J. Buttrey, J.M. Tranquada, G. Shirane, Physical Review B 49 (1994) 9658.
[15] J.A. Alonso, J. Amador, J.L. Martínez, I. Rasines, J. Rodríguez-Carvajal, R. Sáez-Puche, Solid State Communications 76 (1990) 467.
[16] E. Garcria-Matres, J. Rodríguez-Carvajal, J.L. Martínez, A. Salinas-Sánchez, R. Sáez-Puche, Solid State Communications 85 (1993) 553.
[17] E. García-Matres, J.L. Martínez, J. Rodríguez-Carjaval, European Physical Journal B 24 (2001) 59.
[18] M.N. Popova, S.A. Klimin, E.P. Chukalina, E.A. Romanov, B.Z. Malkin, E. Antic-Fidancev, B.V. Mill, G. Dhalenne, Physical Review B 71 (2005) 024414.
[19] M.N. Popova, S.A. Klimin, E.P. Chukalina, B.Z. Malkin, R.Z. Levitin, B.V. Mill, E. Antic-Fidancev, Physical Review B 68 (2003) 155103.
[20] S.A. Klimin, A.S. Galkin, M.N. Popova, Physics Letters A 376 (2012) 1861.
[21] A. Zheludev, J.M. Tranquada, T. Vogt, D.J. Buttrey, Physical Review B 54 (1996) 7210.
[22] S. Maslov, A. Zheludev, Physical Review Letters 80 (1998) 5786.
[23] A. Zheludev, S. Maslov, T. Yokoo, J. Akimitsu, S. Raymond, S.E. Nagler, K. Hirota, Physical Review B 1 (2000) 1601.
[24] A. Zheludev, S. Maslov, T. Yokoo, S. Raymond, S.E. Nagler, J. Akimitsu, Journal of Physics: Condensed Matter 13 (2001) R325.
[25] J.V. Alvarez, Roser Valentí, A. Zheludev, Physical Review B 65 (2002) 184417.
[26] J.V. Alvarez, Roser Valenti, European Physical Journal B 44 (2005) 439.
[27] M.V. Narozhnyy, S.A. Klimin, E.A. Popova, G. Dhalenne, Journal of Rare Earths 27 (2009) 603.
[28] J. Das, A.V. Mahajan, J. Bobroff, H. Alloul, F. Alet, E.S. Sørensen, Physical Review B 69 (2004) 144404.
[29] M.N. Popova, E.A. Romanov, S.A. Klimin, E.P. Chukalina, B.V. Mill, G. Dhalenne, Physics of the Solid State 47 (2005) 1497.
[30] T. Ito, H. Takagi, Physica B: Condensed Matter 329–333 (2003) 890.
[31] E. Janod, C. Payen, F.-X. Lannuzel, K. Schoumacker, Physical Review B 63 (2001) 212406.
[32] V. Villar, R. Mélin, C. Paulsen, J. Souletie, E. Janod, C. Payen, European Physical Journal B 25 (2002) 39.
[33] Z. Hu, M. Knupfer, M. Kielwein, U.K. Rößler, M.S. Golden, J. Fink, F.M.F. de Groot, T. Ito, K. Oka, G. Kaindl, European Physical Journal B 26 (2002) 449.
[34] C.D. Batista, A.A. Aligia, J. Eroles, Physical Review Letters 81 (1998) 4027.
[35] Ian Affleck, Tom Kennedy, Elliott H. Lieb, Hal Tasaki, Physical Review Letters 59 (1987) 799.
[36] E.S. Sørensen, I. Affleck, Physical Review B 49 (1994) 15771.
[37] C.D. Batista, K. Hallberg, A.A. Aligia, Physical Review B 60 (R12) (1999) 553.
[38] F. Tedoldi, R. Santachiara, M. Horvatić, Physical Review Letters 83 (1999) 412.